fibers

MDPI

Review

Granulated Silica Method for the Fiber Preform Production

Sönke Pilz [1,*], Hossein Najafi [1], Manuel Ryser [2] and Valerio Romano [1,2,*]

[1] Institute for Applied Laser, Photonics and Surface Technologies (ALPS), Bern University of Applied Sciences, Pestalozzistrasse 20, CH-3400 Burgdorf, Switzerland; hossein.najafi@bfh.ch

[2] Institute of Applied Physics (IAP), University of Bern, Sidlerstrasse 5, CH-3012 Bern, Switzerland; manuel.ryser@iap.unibe.ch

* Correspondence: soenke.pilz@bfh.ch (S.P.); valerio.romano@iap.unibe.ch (V.R.); Tel.: +41-34-426-4347 (S.P.); +41-31-631-8940 (V.R.)

Academic Editors: Giancarlo Righini, Shibin Jiang and Francesco Prudenzano
Received: 24 April 2017; Accepted: 19 June 2017; Published: 11 July 2017

Abstract: During the past few years, we have studied the granulated silica method as a versatile and cost effective way of fiber preform production and the sol-gel method. Until now, we have used the sol-gel technology together with an iterative re-melting and milling step in order to produce rare earth or transition metal doped granular material for the granulated silica method. Here, we present that the iterative re-melting (laser-assisted) and milling step is no longer needed to reach a high homogeneity. The sol-gel method also offers a high degree of compositional flexibility with respect to dopants; it further facilitates achieving high concentrations, even in cases when several dopants are used. We employed optical active doped sol-gel derived granulate for the fiber core, whereas pure or index-raised granulated silica has been employed for the cladding. Based on the powder-in-tube technique, where silica glass tubes are appropriately filled with these granular materials, fibers has been directly drawn ("fiber rapid prototyping"), or eventually after an additional optional quality enhancing vitrification step. The powder-in-tube technique is also ideally suited for the preparation of microstructured optical fibers.

Keywords: optical fibers; sol-gel; sol-gel-based granulated silica method; preform; power-in-tube preform; large mode area fiber; active fiber

1. Introduction

During the last 15 years, optical fiber has seen a remarkable redefinition of its function and role. The simple concept of a material based index step between core and cladding has been complemented and enhanced by a variety of new concepts such as photonic crystal fibers (PCFs) or large mode area fibers (LMA), just to name the most known concepts. These new concepts have radically changed the potential applications that we associate with a fiber [1–5]. During the last 13 years, we have studied two interesting ways of fiber production starting with the preform [6–20].

The goal of our studies was on the one hand to gain some compositional flexibility in doping the cores of fibers and on the other hand to have some more control over the microstructure of the fiber [6–20]. To reach these two goals, we have been working on the sol-gel method for fiber material production and on the granulated silica method for preform assembly [6–12].

1.1. The Sol-Gel Method

One main benefit of the sol-gel method is that doped silica material of high purity can be produce at temperature below 2000 °C in contrast to the standard methods [11,12,21,22]. Furthermore, the optical material derived from the sol-gel method possesses a high homogeneity (in nano-scale) [8].

Another advantage of the sol-gel method is that it features a high degree of freedom concerning the compositional flexibility [6,7]. This includes not only a higher degree of freedom concerning optically active dopants (e.g., rare earth), optically passive dopants (e.g., phosphorous and aluminum) and its simplicity to incorporate them, but also high dopant concentrations (up to several at. %) can be reached with less effort compared to the traditional glass production [6,7].

For material production, the sol-gel method allows to achieve a homogeneous distribution of the dopants per se since one starts from a liquid mixture [23]. This has been shown in the literature [10,24,25] when the sol-gel method was used to coat the interior of silica tubes, similar to other methods (e.g., MCVD: Modified Chemical Vapor Deposition). In general, using sol-gel as a replacement for MCVD works fairly well if one can accept the intrinsically high amount of OH-groups in the material, which is not a problem for wavelengths up to the NIR (near-infrared) region. However, if the sol-gel method is simply used to coat the interior of the preform tube, one does exploit the compositions freedom of the sol-gel method but not the structural benefits respectively the flexibility of the granulated silica method, e.g., for the production of PCFs (photonic crystal fibers) [23]. The (misleading) assumption that one might create microstructures in order to obtain a microstructured fiber by pouring a precursor solution into a microstructured form and then have an in situ gelatinization is very difficult to achieve, as the solidified sol-gel material is only about 7% of the volume of the starting materials (the rest is evaporated during the solidifying process) [23].

1.2. The Granulated Silica Method

The other method that we have studied is the granulated silica method [14–18]. This method offers unprecedented flexibility with respect to the geometry of the fibers [13,16]. The granulated silica enables the preform assembly based on the powder-in-tube technique, which in turn is resting upon assembling tubes and doped or pure silica granulates [19,20,26–29]. By virtue of this method, we gain versatility in producing any kind of fiber structure since no symmetry is required, inter alia microstructured optical fibers [13,16]. Moreover, it can be regarded as a "fiber rapid prototyping" technique as it can be used to draw fibers without vitrification step directly from silica tubes appropriately filled with granulated silica [6].

In its original variant, this method starts from an oxides mixture of the desired fiber glass components (referred to as oxide-based granulated silica method) [14–18]. Coarse grains of pure silica granulate are mixed with fine dopant powder (e.g., rare earth oxides or transition metal oxides) and co-dopant powder (e.g., aluminum oxide Al_2O_3 or germanium oxide GeO_2) [6,14–18]. This versatility has its price: microbubbles and glass inhomogeneities (e.g., incomplete diffusion) lead to scattering losses of fibers based on this approach in the range of 1–5 dB/m at 632 nm, depending on the doping level [6,14,15]. However, the flexibility of the method is so attractive that several process variants and additional techniques have been developed [14,17,29–32], among others, to obtain more homogeneous glass.

One of these methods is based on an iteratively melting and milling process for the granulated silica (oxide-based and sol-gel-based) to increase the homogeneity [6,9]. However, here we present our recent results ("Homogeneity" in Section 3.1.3) that this iterative melting and milling process it no longer needed to increase the homogeneity of the sol-gel-based granulated silica [7,8]. Another method used the stack-and-draw technique for homogenization [33] and reduced the scattering losses to values as low as 0.1 dB/m (measured at 1100 nm wavelength).

Currently, we are attempting to "merge" the advantages of the sol-gel method, mainly the compositional flexibility, with the structural advantages of the granulated silica method [6,7].

First, a base material is produced by the sol-gel method, which is already doped at the grain level with the needed dopants [6,7]. Next, this material is post-processed to obtain amongst others the desired granulometric distribution [6,7]. A grain size in the range of above 100 µm is desirable as then evacuation of the preform in the drawing furnace allows obtaining prototype fibers of acceptable quality for testing [6,7]. Microbubbles together with other scattering centers, arising from, e.g., not fully

vitrified granulate during fiber drawing, are the major sources for scattering losses. These scattering losses of the fibers can be lowered by inserting an additional vitrification step before drawing [7]. Fibers based on the granulated silica method intrinsically feature higher losses as compared to MCVD or VAD. However, the losses of fibers based on the granulated silica method are low enough in order that these fibers can be used in a fiber laser or fiber amplifier setups, where only a few meter are needed.

Furthermore, the combination of sol-gel method and granulated silica method features also a good control over the refractive index of the material [6,7]. For example, if Aluminum (Al) and Phosphorous (P) are individually used as dopant, the refractive index is increased in each case. However, by simultaneously doping with Al and P, the refractive index can be tailored by the ratio of Al to P, since the Phosphorous can compensate the refractive index change arising from the Aluminum [6,7]. This in turn makes this approach very attractive for the production of fibers such as large mode area (LMA) fibers and leakage channel fibers (LCFs), where a small refractive index contrast between core (LMA) and cladding or core and microstructure (LCFs) is needed. The addition of Phosphorous is also beneficial with respect to the photodarkening [6,7].

2. Oxide-Based Granulated Silica Method

As stated above the most straightforward way to implement the granulated silica method is the oxide-based granulated silica method, starting from a mixture of dry oxides in the composition desired. Pure granulated silica (SiO_2), oxides of the desired rare earth dopant (e.g., Er_2O_3 or Yb_2O_3) and co-dopant elements (to enhance solubility of the rare earths in silica, e.g., Al_2O_3 or P_2O_5) are mixed according to their respective molar concentration. To evenly distribute elements and increase the homogeneity in the glass matrix, the mixture is filled in a graphite box and exposed to a beam of a CO_2-laser operated at several 100 W with an unfocussed beam (the beam diameter is typically in the order of 10 mm) for a time of 15 s–45 s, respectively [6]. With this procedure doped, glass pellets of 1 cm–2 cm diameter are produced. To get a uniform vitrification the back sides of the pellets are also irradiated in a similar way. The produced pellets are then milled with a planetary small ball milling machine for several minutes [6]. This melting and milling process is applied iteratively several times (in most cases 5 times) until the produced pellets show a homogenous and transparent appearance. Finally the pellets are milled to coarse grained powder (granulate) and sieved to the size of usually grain size from 150 µm to 1 mm [6]. The right choice of the coarseness of the granulate material is important to facilitate the evacuation of the preform during the fiber drawing process. The fiber preform assembly is based on the power-in-tube technique and is schematically shown in Figure 1.

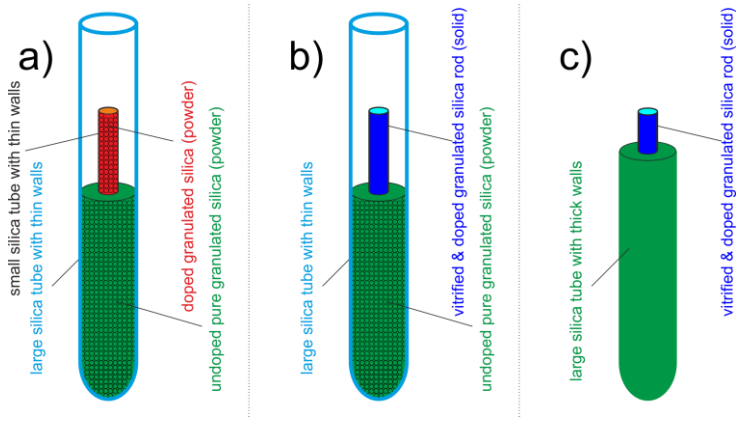

Figure 1. Preform assembly. (**a**) Powder-in-tube technique: smaller silica tube is filled with doped granulated silica and the bigger silica tube is filled with undoped pure granulated silica (SiO_2). Adapted powder-in-tube technique for vitrified core rods where the cladding area of the preform consists of: (**b**) pure silica granulate (SiO_2); or (**c**) solid pure silica [7].

This basic procedure can also be used with metals and transition metals as dopants [17,18]. In this way, a spectrally flat attenuator in the wavelength range between 1250 nm and 1610 nm was obtained [34]. In Reference [35], an example of a produced fiber derived from the oxide-based granulated silica method doped with Nd/Er/Bi/Al is presented. The authors achieved a broadband emission from 1000 nm to 1700 nm. Other examples are scintillator fibers doped with antimony (Sb) or cerium (Ce) for particle beam detection [36]. Growing interest is being shown for bismuth as a dopant [37,38]. Bismuth-doped fibers are expected to eventually develop into a very attractive market to produce extended L-band fiber amplifiers. In addition, bismuth-based erbium-doped optical fiber allows for extended L band and C + L band.

The oxide-based granulated silica method has shown the basic feasibility of such fibers [17,18], however, at the cost of high background losses deriving from scattering.

3. Sol-Gel-Based Granulated Silica Method

3.1. Ytterbium Doped and Aluminum and Phosphorous Co-doped Fiber Manufactured by the Sol-Gel-Based Granulated Silica Method

3.1.1. The Sol-Gel Method

The sol-gel process starts from a liquid condition by mixing an alkoxide precursor (TEOS) with, e.g., dissolved salt precursors (dopants) at room temperature [6,7]. The basic principle of the sol-gel process is shown in Figure 2 [7]. Through the addition of distilled water and stirring at moderated heat this solution (sol) undergoes hydrolysis, condensation and finally gelatinization. The sol has transformed into a gel after the gelatinization. This gel is then dried into a power, where every powder grain is doped [7].

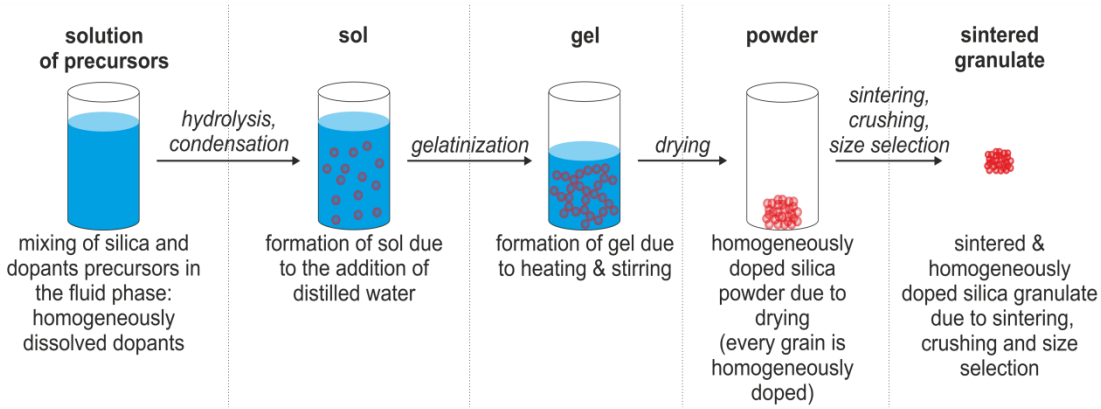

Figure 2. Basic principle of the sol-gel process [7].

Subsequently, we apply several different post-processing steps in order to use the powder and the final granulate together with a slightly adapted powder-in-tube preform assembly for fiber drawing [7]. In a first post-processing step, the powder is sintered into a block of powder [6,7]. During the sintering process, most of the OH-groups, which are intrinsically present in the granulate derived from the sol-gel process, are eliminated. However, residual OH-groups can be another reason for the background losses. The influence and reduction of OH-groups is still under investigation. Subsequently, this block of powder is then crushed into a granulate. By sieving this granulate, we can select the grain size of the granulate and its distribution [6,7]. This granulate can now be used directly ("fiber rapid prototyping") for an adapted powder-in-tube technique or in corporation with an additional vitrification step [6,7]. The iterative CO_2-laser treatment of melting and subsequently milling, which we reported, inter alia in [6], is no longer needed to improve the homogeneity [7,8] of the granulate derived from sol-gel. This CO_2-laser treatment was introduced to improve the homogeneity for the oxide-based granulated silica

method (direct mixing of oxides; not sol-gel based) and which was taken over for the sol-gel-based granulated silica method in the beginning of our work [6,9]. For a detailed analysis of the homogeneity please check "Homogeneity" in Section 3.1.3 or [8].

3.1.2. Vitrification, Preform Assembling and Fiber Drawing

We can used the sol-gel derived granulate directly without any vitrification step for the preform assembly, which we call "fiber rapid prototyping" [6,14–18] (see Figure 3) [7]. For that, we usually place a smaller silica tube (depending on the core to cladding ratio of the final fiber) in a larger silica preform tube (17 mm × 21 mm) [6,14–18]. The smaller tube is then filled with the doped granulate derived from the sol-gel process, which will become the core of the fiber. The intermediate space is filled with pure silica powder (SiO_2), which will become the cladding of the fiber [6,14–18]. Alternatively, we can also use a preform tube with thick pure silica walls as a large preform, where the cavity of this tube replaces the smaller silica tube and can filled directly with the granulate [6,9]. In this configuration, the filled cavity will become the core, whereas the thick silica walls will become the cladding of the fiber [6,9]. The authors are aware of the diffusion between core and cladding regions during fiber drawing, however it was not yet analyzed, since our focus was on the homogeneity. As mentioned before, the grain size and size distribution of the granulate plays an important role for the evacuation of the preform during fiber drawing for the "fiber rapid prototyping" and for the additional vitrification step. The level, density and size of microbubbles depend on granulate parameters such as grains size and size distribution as well as on the preform diameter and the applied vacuum. For "fiber rapid prototyping", we use coarse granulate (usually grain size from 150 µm to 1 mm) [6]. The fibers produced by "fiber rapid prototyping" suffer from high propagation and scattering losses in the range 0.75 dB/m to 5 dB/m at 633 nm due to, e.g., microbubbles [6,14,15].

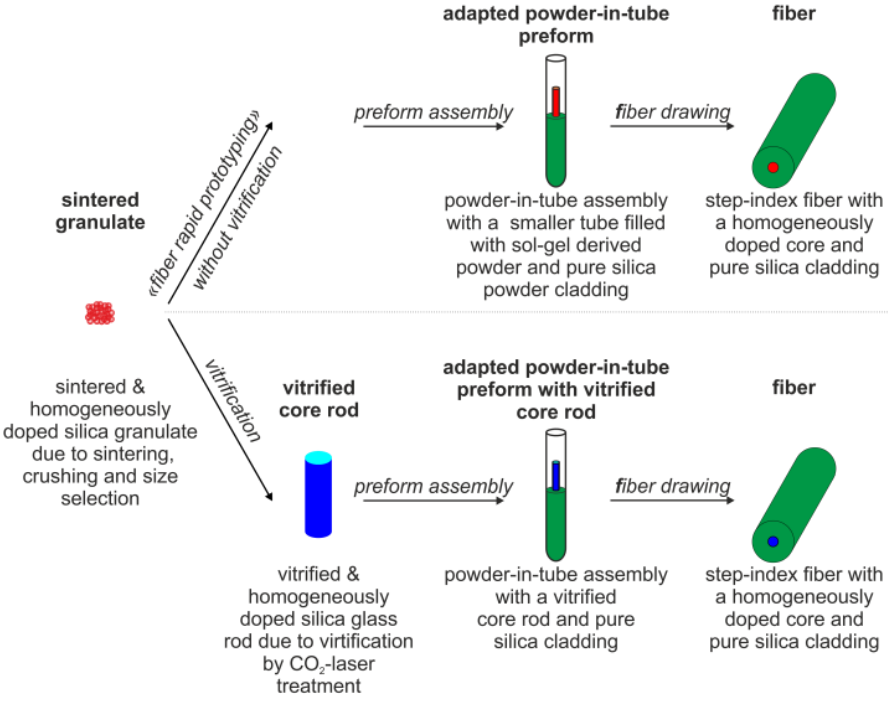

Figure 3. Overview of our preform assembly, fiber drawing and additional vitrification [7].

By using an additional vitrification step for the sol-gel derived granulate before preform assembly, the scattering and propagation losses of the final fiber can be reduced [7]. We can vitrify the granulate into a solid glass rods with a diameter up to 5 mm, which we referred to as vitrified core rods (shown in Figure 4) [7]. These vitrified core rods can be used for the two before mentioned adapted

powder-in-tube preform assembly version (preform cladding region consists either of pure silica powder or solid pure silica glass), where the vitrified core rod replaces the doped granulate in the center of the preform, shown in Figure 1b–c) [7].

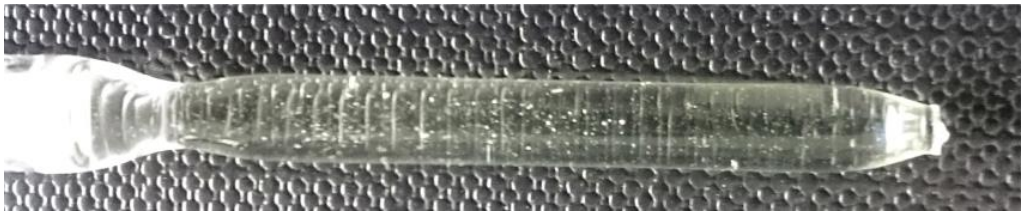

Figure 4. Vitrified core rod after vitrification treatment (diameter < 5 mm) [7].

After the preform assembly based on the adapted power-in-tube technique, the preform is drawn into fiber at a temperature in the range of 1900 °C–2000 °C. If the preform consists of granulate or a powder area, then the preform is additionally evacuated from the top.

3.1.3. Yb/Al/P Doped Sol-Gel-Based Granulated Silica

Here, we present the results of our sol-gel-based granulated silica method doped with Ytterbium (Yb) and co-doped with Aluminum (Al) and Phosphorous (P) [7]. The rare earth element Ytterbium is the optical active dopant element, which features an emission in the near infrared region of 1000 nm–1100 nm and can be excited by commercial pump diodes at 976 nm or in the range of 915 nm, see Figure 5 [7]. Aluminum is used to increase the solubility of the Ytterbium in the sol-gel process (hold true for all rare earth elements) and to prevent the clustering of the Ytterbium (hold also true for all rare earth elements) [6]. Phosphorous is primarily used to reduce photo darkening. Furthermore, when Al and P are individually applied, each of the two elements on its own would increase the refractive index, when applied in combination, the Phosphorous can compensate the refractive index change arising from the Aluminum [6,7]. Thus, by tailoring the ratio of Al to P, we can control the refractive index.

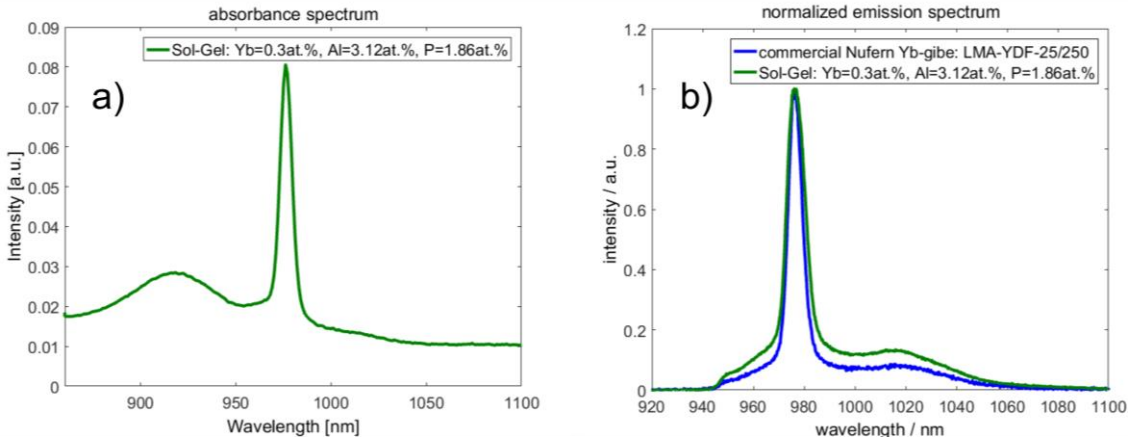

Figure 5. (**a**) Absorbance spectrum of the self-made sol-gel based fiber; and (**b**) emission spectra: self-made sol-gel based fiber and commercial Yb doped fiber (Nufern: LMA-YDF-25/250) [7].

As silica precursor we used liquid tetraethyl orthosilicate TEOS: $Si(OC_2H_5)_4$ [6,7]. For the dopants, the following precursors were used in powder form: ytterbium (III) nitrate pentahydrate ($Yb(NO_3)_3 \cdot 5H_2O$), aluminum nitrate nonahydrate ($Al(NO_3)_3 \cdot 9H_2O$) and phosphorus pentoxide (P_2O_5) [6,7]. Before mixing all precursors together, the powdery precursors and TEOS are separately solved in ethanol. The combination of all precursors and ethanol is then stirred at room temperature

(see Figure 2) [6,7]. If the pH level of this solution is not yet below 6, hydrochloric acid (HCl) is used as a catalyst to lower the pH value below 6. Under the addition of deionized water and supplementary moderate heating (70 °C–80 °C), the mixed solution undergoes hydrolysis followed by condensation and gelatinization. The transformation from a solution into a gel takes a couple of hours. The resulting gel is then dried into a powder, where every grain of the powder is doped [6,7]. Subsequently, the drying of the gel into a powder is followed by a sintering routine. During this sintering routine [6,7], the powder is slowly (2 C°/min) heated up to 1550 °C and kept at this temperature for several hours. Afterwards, the powder is cooled down to room temperature with the same rate (2 C°/min). Furthermore we transformed the loose powder into a block of powder by applying this sintering routine. This block of powder is then crushed into a granulate and, by sieving this granulate, we can select different grain sizes and size distributions [6,7]. It has to mentioned that the crystalline structure of the granulate, which arises during the sintering process, is completely removed and changed into an amorphous structure during fiber drawing in a temperature range above 1900 °C [6,9]; for more details check the "Homogeneity" in Section 3.1.3.

Previously, we reported [6] the direct usage of this granulate together with the power-in-tube preform assembling for the "fiber rapid prototyping". However, the manufactured fibers based on "fiber rapid prototyping" suffered from high scattering and propagation losses (0.75 dB/m to 5 dB/m at 633 nm) [6,14,15]. By using an additional vitrification, these losses can be reduced [7].

Based on two vitrified core rods, we assembled two different large mode area (LMA) preforms [7]. One of these preforms consist of a cladding are made out of pure silica granulate (SiO_2), whereas the other preform consists of a solid pure silica cladding area (see Figure 1) [7]. For the first mentioned preform assembly, the vitrified core rod (diameter of ≈5 mm) was centered in a larger silica tube (inner-/outer-diameter: 17 mm × 21 mm) and the remaining space was filled with pure silica granulate (SiO_2). For the second preform assembly, the vitrified core rod (diameter of < 5 mm) was placed in a pure silica tube with thick walls (inner-/outer-diameter: 5 mm × 20 mm). During fiber drawing, different coatings were applied for the two preforms. For the preform with the granulate cladding area, we applied a high index coating, resulting in a single-clad (SC) fiber, whereas, low index coating was applied for the other preform leading to a double-clad (DC) fiber [7].

(1) Composition

Here, we present our results based on the sol-gel approach. The detailed element doping ratio in atomic percentage (at.%) is shown in Table 1 [7].

Table 1. Element doping ratio in atomic percentage [7].

Element	at. %
Si	94.72
Yb	0.30
Al	3.12
P	1.86

If we account for the valences of the dopant element in the precursors, this leads us to a sol-gel precursor ratio, which is presented in Table 2 and which is indicated this time by the molar percentage (mol.%).

Table 2. Sol-gel precursor ratio in molar percentage.

Sol-Gel Precursor	mol.%
TEOS	95.61
$Yb(NO_3)_3 \cdot 5H_2O$	0.30
$Al(NO_3)_3 \cdot 9H_2O$	3.15
P_2O_5	0.94

After the vitrification, the sol-gel derived material was analyzed by energy-dispersive X-ray spectroscopy (EDX) (Oxford Instruments, Abingdon, UK) of a scanning electron microscope (SEM) (Carl Zeiss Microscopy GmbH, Jena, Germany). The EDX spectrum and the corresponding mass percentages (m. %) are shown in Figure 6 and Table 3. By neglecting the oxygen (O), we calculated the atomic percentages (at. %) (Table 4). The differences between the theoretical precursor mixing ratio (Table 1) and the measured dopant ratio of the vitrified glass (Table 4) can be explained within the accuracy of the EDX [7]. Furthermore a small error in the m. % will lead to a large error in the at. %. We previously concluded [7], based on these EDX measurements and its accuracy, that the composition is conserved during the sol-gel process, the post-processing and even fiber drawing. However, we must confirm this assumption based on additional and more accurate measurements techniques. To do this, we have planned to measure the composition of the sol-gel derived material with wavelength dispersive X-ray fluorescence (WDXRF). If we find, based on the WDXRF analysis, that the doping concentrations are not precisely conserved during the whole process, the concentration changes should be reproducible so that we can tailor the doping concentrations of the final fiber by adjusting the doping concentrations for the precursors.

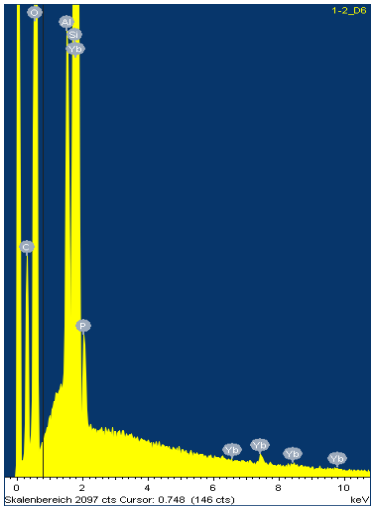

Figure 6. EDX spectrum from sol-gel derived vitrified glass. The carbon (C) peak is due to the carbon-coating applied for EDX sample preparation [7].

Table 3. EDX measurement: Element doping ratio in mass percentage (including oxygen).

Element	m. %
Si	34.14
Yb	0.20
Al	1.03
P	0.74
O	63.88

Table 4. EDX measurement: Element doping ratio in atomic percentage (excluding oxygen).

Element	at. %
Si	94.53
Yb	0.56
Al	2.86
P	2.05

(2) Homogeneity

As mentioned above, the granulated silica derived from the sol-gel process was implemented for fabrication of Ytterbium-doped active fibers [7]. The detailed sol-gel process and post-processing was already described in other subsections before, however it must be highlighted that no iterative CO_2-laser treatment of melting and milling to increase the homogeneity is used anymore (in contrast to [6,9]). The structure and homogeneity of the fiber cores were observed by means of scanning electron microscopy and scanning/transmission electron microscope (S/TEM), using a FEI Titan Themis S/TEM (80 kV–300 kV) (FEI, Hillsboro, OR, USA) [8]. The different feature of STEM compared to conventional TEM is that it can focus the electron beam into a narrow spot, which is scanned over the sample and diffracted electrons can be detected by different detectors (see Figure 7) [39]. Various types of contrast in the image and different observation modes including bright field, high angle annular dark-field (HAADF), diffraction pattern, EDX, and high-resolution contrast have been employed. Indeed, scanning transmission electron microscopy (STEM-EDX) provides information in nano-scale chemistry and homogeneity while selected area electron diffraction mode gives information about material amorphization during the process [8].

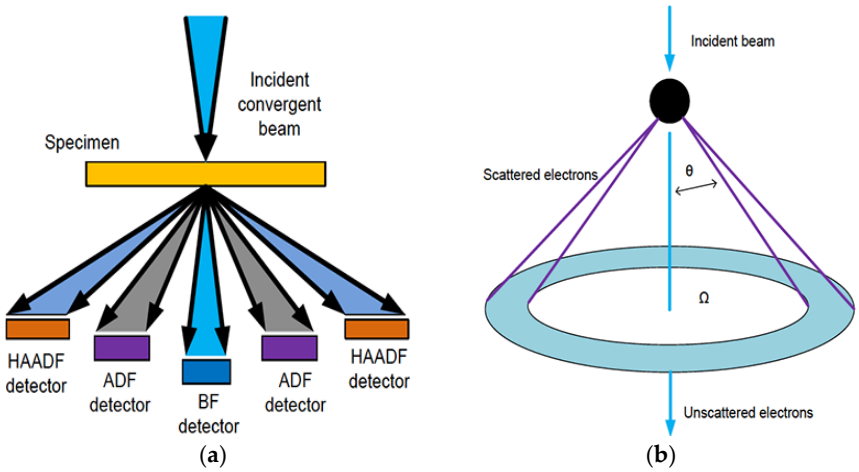

Figure 7. (**a**) Schematic of the HAADF, conventional annular dark-field (ADF) and BF detectors in a STEM; and (**b**) electron scattering by a single isolated atom in STEM [39].

Figure 8 demonstrates the TEM micrographs (BF) showing the nanostructure and diffraction patterns of a fiber core produced by granulated silica derived from the sol-gel process [8]. A well-developed amorphous structure is observed in the fiber core and the electron diffraction pattern shows diffused rings as would be expected for an amorphous phase. However, the question regarding the homogeneity and elemental distribution of the dopant (Yb) and co-dopants (i.e., P and Al) in nano and atomic scales arises. For this purpose, as described previously, STEM was implemented to investigate the fiber core if it is structured into ultra fine substructures, clusters or nano phase segregations. An ultra precise chemical mapping was performed to individualize the different chemical phases, even if they are restricted to ultra small quantities where we have an electron beam with a HAADF STEM resolution of 0.18 nm [8]. Figure 9 demonstrates the elemental distribution images associated with Si, O, P, Al, and Yb, respectively. It can provide useful information on the dopant and co-dopants localization in the nanostructure. It is noteworthy that an extremely homogeneous distribution of dopants is observed in the structure in nano-scale (see Figure 9d–f) [8]. In order to obtain a clue of dopants homogeneity in atomic scale, Figure 10 shows acquired HAADF image in an extremely high magnification. According to the "Z contrast" imaging theory, the brightness of each dot in the STEM-HAADF image mode is roughly proportional to the Z^2 where Z is atomic number [40].

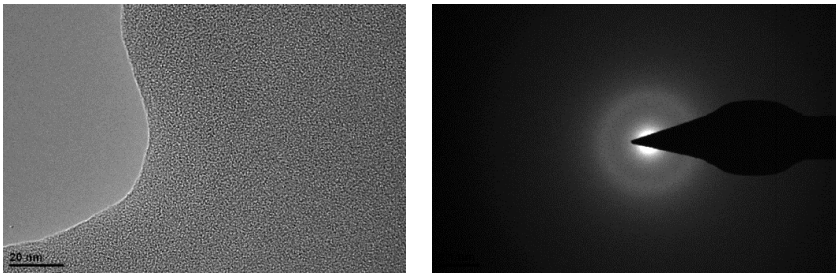

(**a**) (**b**)

Figure 8. TEM micrograph showing the nanostructure and diffraction pattern of a fiber core produced by granulated silica derived from the sol-gel process [8]. (**a**): Bright field image; (**b**): Diffraction pattern.

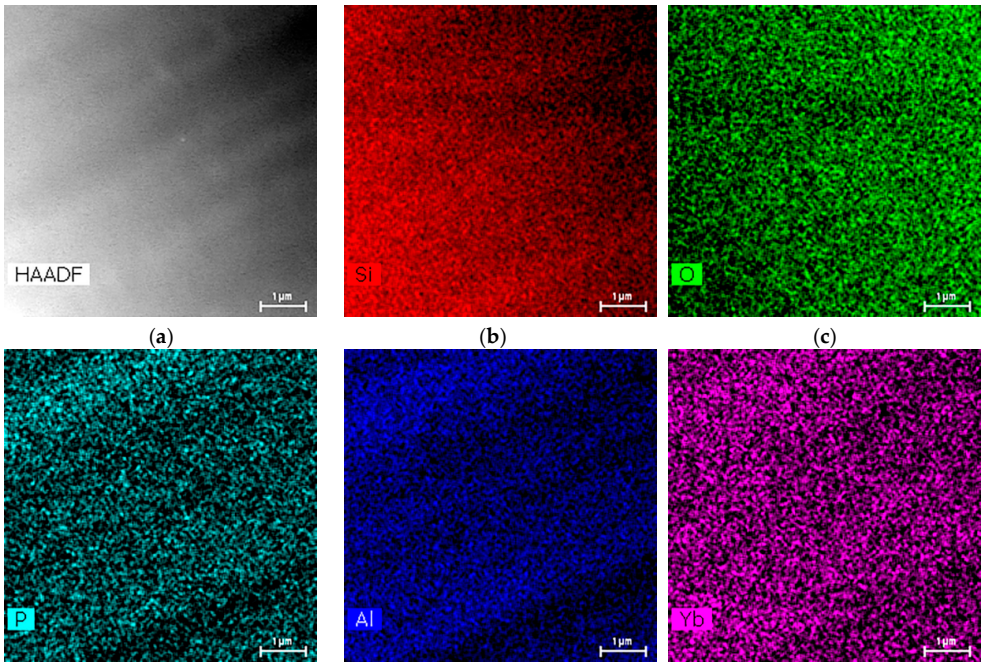

(**a**) (**b**) (**c**)

(**d**) (**e**) (**f**)

Figure 9. STEM micrograph showing the nanostructure and elemental distribution a doped fiber core produced by granulated silica derived from the sol-gel process [8]. (**a**): HAADF image; Chemical mapping of (**b**): Silicon; (**c**): Oxygen; (**d**): Phosphorous; (**e**): Aluminum; (**f**): Ytterbium.

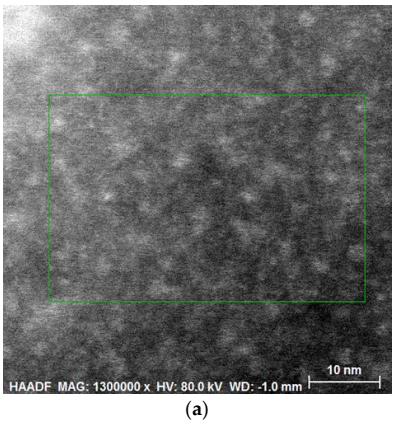

(**a**)

Figure 10. *Cont.*

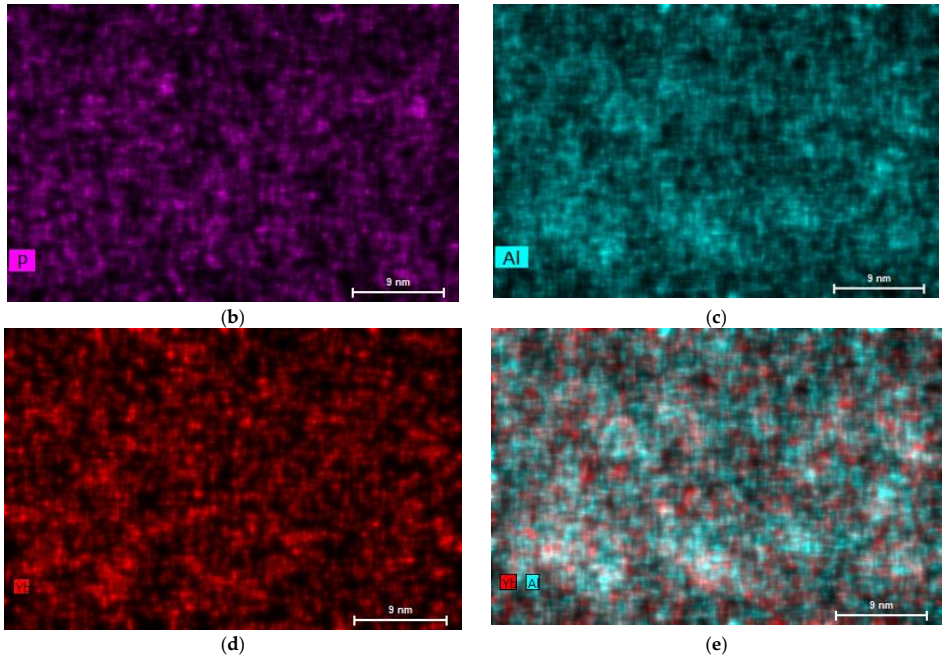

Figure 10. (**a**) HAADF-STEM micrograph; and (**b**–**d**) elemental mapping acquired at ultra-high magnification from a fiber core [8]. (**e**): Al and Yb chemical mapping.

Considering the rational hypothesis of a flat investigated area within the field of view at such high magnification, we can conclude that the bright areas on the micrographs in Figure 10a represent Yb atoms and clusters since the Yb atom species are the only heavy dopant in the core [8]. The atomic numbers of other elements and dopants (i.e., Al, P, Si, and O) are much lower than Yb. Furthermore, Figure 10a) shows that at such atomic scale magnification, some Yb atoms tend to cluster together while some are randomly distributed in the core. Given the fact that Yb ionic diameter is around 0.5 nm and the average cluster size in the observation area is around 4 nm [8]. Consequently, it can be concluded that Yb clusters are formed by an average of eight atoms or, in other words, Yb clusters are formed by less than 10 atoms in 2D scale [8].

According to the best knowledge of the authors, it is a valuable achievement of the present work. In order to validate this hypothesis, the EDX spectrum was performed in both suspected clustered area and free cluster zone (see Figure 11) [8]. The green color shows the EDX spectrum of the clustered area, while the blue spectrum indicates that of the free cluster area. The strong Si and O signals come from the fiber host, SiO_2. The Cu signals come from the copper grid holder supporting the TEM specimen of the fiber.

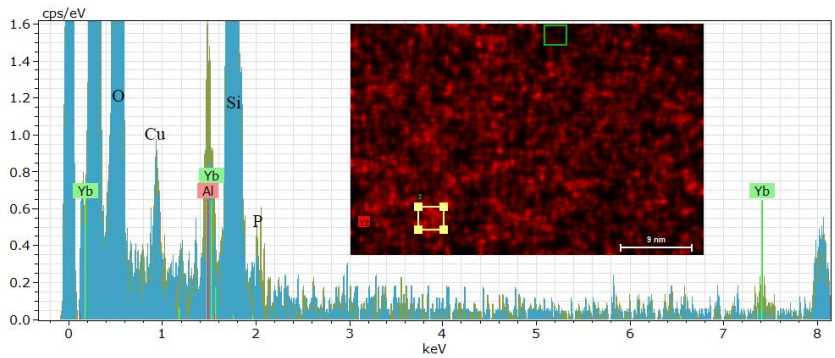

Figure 11. EDX spectra from a clustered area (green) and a free cluster zone (blue): the visible signal from Yb atoms within the clustered area [8].

The only distinction in the two spectra is the visible signal from Yb elements within the clustered area. It results in the dominating contrast (Figure 10a) in STEM-HAADF image given its larger atomic number, Z.

In conclusion, a great progress in homogeneity could be achieved in the granulated silica derived from the sol-gel process (without any iterative CO_2-laser treatment of melting and milling) compared to the oxide-based approach, as shown in Figure 12 [7]. The fiber core derived from the sol-gel process exhibits a matrix with clear natural and homogenous distribution of dopants and co-dopants, while the core derived from the oxide-based granulated silica approach shows nano segregations containing a range of hydrated and nano-crystalline polymorphs in the matrix. Then, we conclude that the granulated silica derived from the sol-gel process is an extremely powerful technique for fabrication of Ytterbium-doped active fibers in terms of homogeneity of dopants and co-dopants [8].

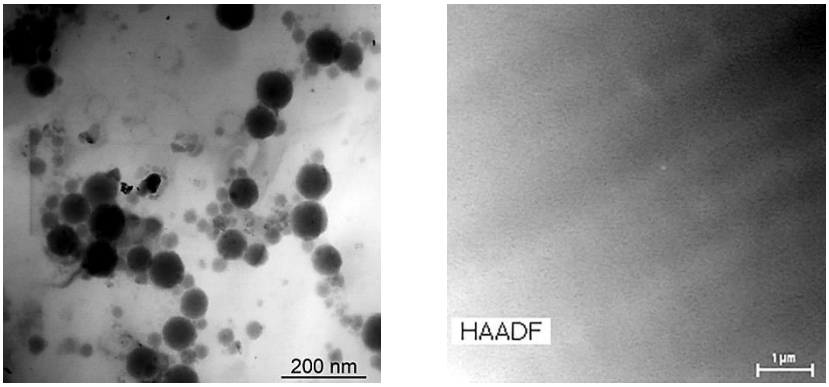

(**a**) (**b**)

Figure 12. Progress in homogeneity from: (**a**) oxide-based; to (**b**) sol-gel-based granulated silica method [7].

(3) Absorption and Emission Spectra, Lifetime

The absorbance spectrum of a vitrified, 1 mm-thick, plane-parallel plate was measured by a Perkin Elmer Lambda 750 spectrometer (Perkin Elmer, Waltham, MA, USA) (Figure 5a) [7]. The sol-gel derived material features the well-known Ytterbium absorption characteristics and thus corresponds well with the absorption spectra of commercial Yb doped fibers. Therefore, we can use the standard pumping wavelengths for Yb doped fibers at 976 nm or in the region of 915 nm [7].

The emission spectrum was recorded under an excitation at 915 nm and by an Ocean Optics USB4000 spectrometer (Ocean Optics, Dunedin, FL, USA) [7]. The emission spectrum of our self-made sol-gel based fiber corresponds well to the emission spectrum of a commercial Yb-doped fiber (Nufern: LMA-YDF-25/250) (Nufern, East Granby, CT, USA) (Figure 5b).

The average lifetime of the upper state laser level of the Ytterbium of vitrified core rods was determined to be 0.99 ms (theoretical value of 1 ms) [7], whereas self-drawn fibers based on these vitrified core rod feature a lifetime of 0.75 ms–0.8 ms, which corresponds well with the measured lifetime of a commercial Yb doped fiber (Liekki: Yb1200-25/250: 0.8 ms) (nLight, Vancouver, WA, USA). A bigger change in lifetime would indicate quenching and clustering of the Yb atoms [7].

3.1.4. Yb/Al/P Doped Sol-Gel-Based Granulated Silica Fibers

As mentioned before, we manufactured two different large mode area (LMA) fibers with different preform assembly and different coatings (high and low index coating) [7].

(1) Single-Clad Fiber: Δn and Scattering Losses [7]

The single-clad fiber was produced based on a preform with vitrified doped core rod (derived from the sol-gel process) and an undoped pure silica granulate cladding area (see Figure 13a). High refractive index coating was applied during fiber drawing, resulting in a single-clad (SC) fiber with the fiber geometry found in Table 5.

Table 5. Geometry parameters of the self-made single-clad [7].

Core diameter:	20 µm
Cladding diameter:	190 µm
Coating:	High index
Coating diameter:	400 µm

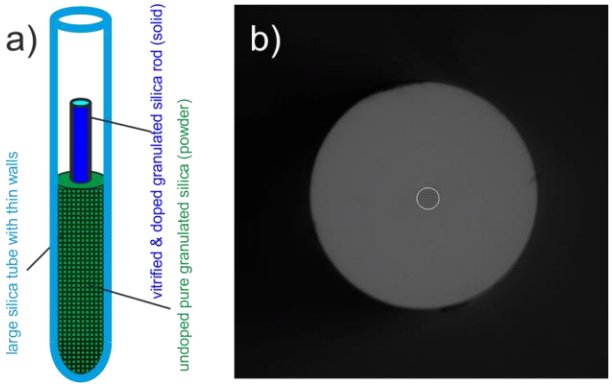

Figure 13. Single-clad (SC) LMA fiber derived from sol-gel granulated silica method: (**a**) preform assembly; and (**b**) fiber geometry: microscope image (white ring indicates the core) [7].

Based on this single-clad fiber, we measured the refractive index contrast between undoped cladding and doped core and the scattering losses of the core. In order to determine the refractive index contrast, we use on the one hand a self-built reflection based refractive index mapping setup [41] and on the other hand a self-built inversed refracted near-field (IRNF) setup [42,43]. The first mentioned setup is very time consuming (scanning) and accurate, whereas the second setup is based on a fast imaging technique but does not feature the same accuracy.

The refractive index profile of the SC LMA fiber for the reflection-based setup is shown in Figure 14. The core and cladding averages are obtained by averaging a large area of the core and the cladding region, respectively, in contrast to the line scan [7]. Based on the averaged value, the refractive index contrast between the doped core and pure silica cladding (derived from pure silica granulate preform cladding area) is $\Delta n = 3.35 \times 10^{-3}$ (confirmed also by IRNF setup) [7]. If we assume a refractive index of 1.45 for the pure silica cladding, this leads to a NA of 0.0986 (commercial LMA fibers normally feature a NA (numerical aperture) of 0.07–0.08). However, by tailoring the doping concentration for Phosphorous, we have the possibility to adjust the refractive index contrast and the NA.

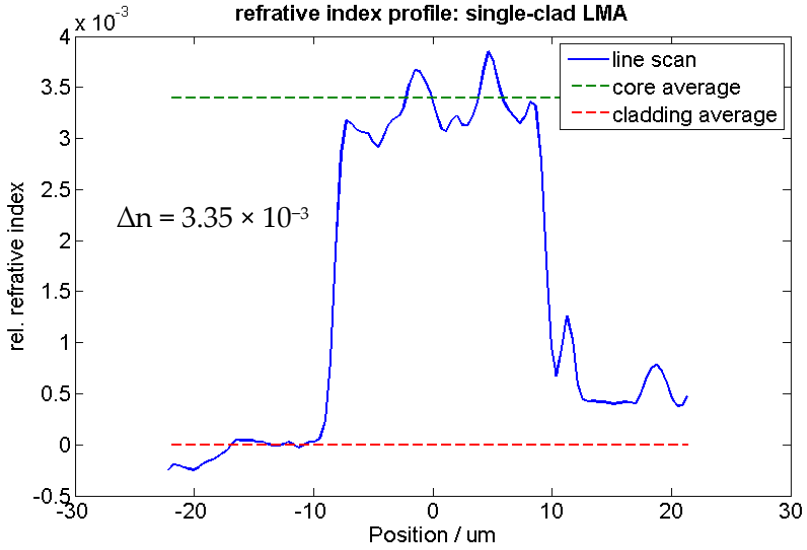

Figure 14. Reflection-based refractive index mapping method [41]: refractive index profile of the single-clad fiber with a Δn of 3.35 × 10^{-3} [7].

Based on this single-clad fiber, we could determine the propagation resp. scattering losses of the fiber core derived from sol-gel, since the fiber core is the only waveguide. In order to do that, we used two diverse methods at two different (not absorbing) wavelengths. On the one hand, we used the destructive cutback method at 633 nm and on the other hand we used a self-built and non-destructive high-resolution optical time-domain reflectometer (HR-OTDR) at 1550 nm [44]. For the cutback method, we obtained propagation/scattering losses of 0.2 dB/m at 633 nm and, for the HR-OTDR, we measured losses of 0.02414 dB/m at 1550 nm [7]. The main source for these losses is scattering and not absorption, since wavelengths at non-absorbing wavelength have been used for theses setups. The estimated losses in the near infrared region of interest (1000 nm–1100 nm), if no absorption at these wavelengths is take into account, is low enough to use these sol-gel-based fibers in laser or amplifier setups and applications [7].

(2) Double-Clad Fiber: Δn

The double-clad fiber was produced based on a preform with vitrified doped core rod (derived from the sol-gel process) and an undoped pure silica solid cladding area (see Figure 15a). Low refractive index coating was applied during fiber drawing, resulting in a double-clad (DC) fiber with the fiber geometry found in Table 6.

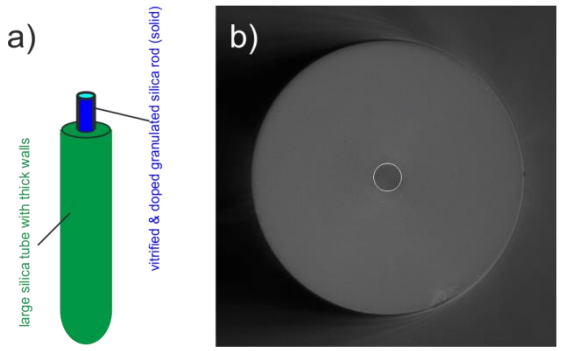

Figure 15. Double-clad (DC) LMA fiber derived from sol-gel granulated silica method: (**a**) preform assembly; and (**b**) fiber geometry: microscope image (white ring indicates the core) [7].

Table 6. Geometry parameters of the self-made double-clad fiber [7].

Core diameter:	22 µm
Cladding diameter:	250 µm
Coating:	Low index
Coating diameter:	400 µm

The refractive index profile of the DC LMA fiber for the reflection-based setup is shown in Figure 16. Based on the averaged value, the refractive index contrast between the doped core and pure silica cladding (derived from solid pure silica preform cladding area) is $\Delta n = 2.65 \times 10^{-3}$ (confirmed also by IRNF setup) [7]. If we assume a refractive index of 1.45 for the pure silica cladding, this leads to a NA of 0.0877.

For the single-clad fiber, we used a preform cladding area made out of pure silica granulate, whereas, for the double-clad fiber, a solid pure silica cladding preform area was used. The granulated silica and solid silica cladding feature a slightly different refractive index, which in turn can explain the slight differences in refractive index contrast and NA of the self-made single-clad and double-clad fibers [7].

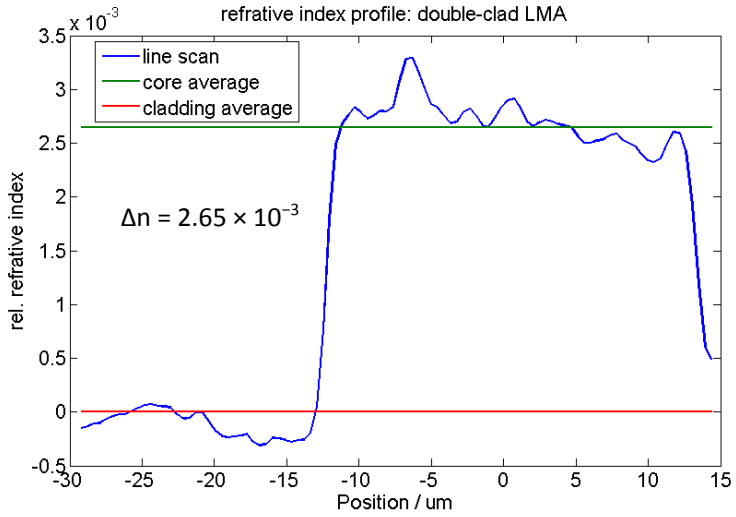

Figure 16. Reflection-based refractive index mapping method [41]: refractive index profile of the double-clad fiber with a Δn of 2.65×10^{-3} [7].

Based on this double-clad fiber, lasing and amplification tests are in progress. Furthermore, different fiber geometries and configuration (SC, DC round cladding, DC octagonal cladding) are planned for testing.

3.2. Other Sol-Gel-Based Granulated Silica Compositions

3.2.1. High P Content for Yb/Al/P Doped Sol-Gel-Based Granulated Silica

Based on the above-presented Yb/Al/P doped sol-gel-based granulated silica, we also tested high dopant concentrations for all the three doping elements. Although we successfully tested high doping concentration up to several at. % for all of the three dopants, here we exemplarily present one of these tests with a high Phosphorous content, demonstrating the proof of principle. Table 7 shows the results from the EDX measurement based on self-made doped granulate with high P content (and not on a vitrified glass sample) [7]. Compared to Table 4, one can see a strong increase in the P concentration. Thus, we can confirmed that high doping concentration for the (co-)dopants up to several at. % can be reached by the sol-gel-based granulated silica approach.

It has to be mentioned that, for Yb doping, a 6–10 times higher Al concentration is needed in order to prevent the Yb from clustering, which will limit the Yb concentration at some point.

Table 7. EDX measurement: Element doping ratio in atomic percentage (excluding oxygen) for a powder derived from sol-gel with high P content [7].

Element	at. %
Si	89.41
Yb	0.40
Al	3.39
P	6.88

3.2.2. Optical Passive Sol-Gel-Based Granulated Silica

For optical passive dopants, we tested Germanium (Ge) and Titan (Ti) and separately the two co-dopants Aluminum (Al) and Phosphorous (P) we used for the Yb/Al/P doped sol-gel-based granulate [7]. We succeeded in incorporating all of these dopants by the sol-gel-based granulated silica method, which in turn confirms the proof of principle [7]. Figure 17 shows different passively doped droplets (vitrified glass samples) from a preform. Depending on the dopant, the melting temperature is changed, which explains the different shapes of the droplet for a fixed drawing temperature above 1900 °C. Based on these tests, we can confirm the high degree of freedom (and simplicity) concerning the optically passive dopants for the sol-gel-based granulated silica method.

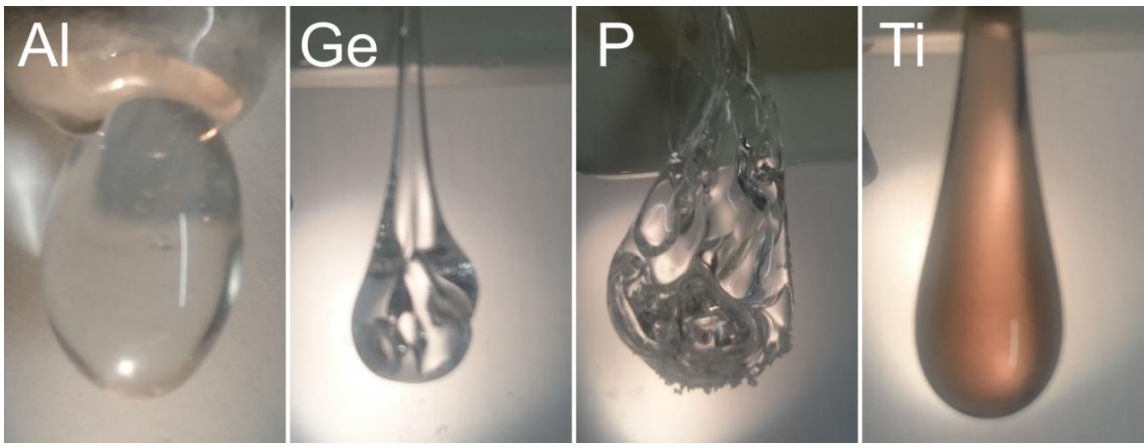

Figure 17. Optical passively separately doped Al, Ge, P and Ti droplets confirm the proof of principle for the sol-gel-based granulated silica method. The different shapes can be explained by a change of melting temperature depending on the dopant (the preforms were drawn at a fix temperature above 1900 °C) [7].

4. Conclusions and Outlook

We have shown that the granulated silica method can be regarded as a rapid fiber production method. The fibers that are produced without further provisions show high scattering losses in the order of 1 dB/m. We assume that these losses derive from microbubbles and scattering at non-fully vitrified grain boundaries. By iterative milling and re-melting, these losses can be reduced to the order of 0.35 dB/m for short fiber pieces.

However, we have found a better way to reduce the background losses of the method while keeping its advantages in versatility of dopant composition and flexibility of defining a fiber structure: the sol-gel method is used to obtain material uniformly doped down to the grain level. When combined with an additional vitrification step before preform assembly, fibers with typical losses of 0.2 dB/m (measured at 633 nm) can be obtained.

The potential of the method has yet to be exploited. At present, passive and active microstructured fibers produced by the sol-gel granulated silica method are under investigation [13]. These will fully exploit the potential of this method.

Acknowledgments: We are very thankful to Thomas Feurer, Willy Lüthy, Loredana DiLabio, Ruth Renner, Bettina Wilhelm, Martin Locher, and Martin Neff for active help in drawing the fibers and discussions. Many thanks also to David Kummer, Stefan Berger and Georgios Karametaxas for their help in sol-gel material production. This work has been carried out over the last 10 years and has involved many technicians and students of the Institute of Applied Physics of the University of Bern IAP whom we also thank. It has been partly financially supported by the Swiss Commission for Technology and Innovation CTI under project 7864.2 and the Swiss National Science Foundation under grant 200020-121663/1.

Author Contributions: V.R. and S.P. conceived and designed the experiments; S.P. performed the sol-gel experiments; S.P. and M.R. performed the fiber-drawing and fiber characteristics; H.N. analyzed the material regarding its homogeneity (S/TEM) and composition (EDX). S.P., H.N., M.R. and V.R. wrote the paper.

Conflicts of Interest: The authors declare no conflict of interest.

References

1. Knight, J.C. Photonic crystal fibers. *Nature* **2003**, *424*. [CrossRef] [PubMed]
2. Birks, T.A.; Knight, J.C.; Russell, P.S. Endlessly single-mode photonic crystal fibre. *Opt. Lett.* **1997**, *22*. [CrossRef]
3. Russell, P.S. Photonic-Crystal Fibers. *J. Lightwave Technol.* **2006**, *24*. [CrossRef]
4. Poli, F.; Cucinotta, A.; Selleri, S. *Photonic Crystal Fibers: Properties and Applications*; Springer: Berlin/Heidelberg, Germany, 2007; Volume 102, ISBN 978-1-4020-6326-8.
5. Bjarklev, A.; Broeng, J.; Bjarklev, A.S. *Photonic Crystal Fibres*; Springer: Berlin/Heidelberg, Germany, 2003; ISBN 978-1-4615-0475-7.
6. Romano, V.; Pilz, S. Sol-Gel based doped granulated silica for the rapid production of optical fibers. *Int. J. Mod. Phys.* **2014**, *28*. [CrossRef]
7. Pilz, S.; Najafi, H.; El Sayed, A.; Boas, J.; Kummer, D.; Scheuner, J.; Etissa, D.; Ryser, M.; Raisin, P.; Berger, S.; et al. Progress in the fabrication of optical fibers by the sol-gel-based granulated silica method. In Proceedings of the SPIE: Microstructured and Specialty Optical Fibres, Brussels, Belgium, 3 April 2016. [CrossRef]
8. Najafi, H.; Pilz, S.; El Sayed, A.; Boas, J.; Kummer, D.; Romano, V. Atomic-scale imaging of dopant atoms and clusters in Yb-doped optical fibers. In Proceedings of the SPIE: Microstructured and Specialty Optical Fibres, Brussels, Belgium, 3 April 2016. [CrossRef]
9. Etissa, D.; Neff, M.; Pilz, S.; Ryser, M.; Romano, V. Rare earth doped optical fiber fabrication by standard and sol-gel derived granulated oxides. In Proceedings of the SPIE: Microstructured and Specialty Optical Fibres, Brussels, Belgium, 16 April 2012. [CrossRef]
10. Pedrazza, U.; Romano, V.; Luethy, W. Yb^{3+}:Al^{3+}:Sol-gel silica glass fiber laser. *Opt. Mater.* **2007**, *29*, 905–907. [CrossRef]
11. Michel, D.; Locher, M.; Lüthy, W.; Romano, V.; Weber, H.P. Tunability of a Nd^{3+}:Al^{3+}:Sol-gel glass fibre laser. In Proceedings of the EPS-QEOD Europhoton Conference on Solid-State and Fiber Coherent Light Sources, Lausanne, Switzerland, 20 August–3 September 2004.
12. Locher, M.; Romano, V.; Lüthy, W.; Weber, H.P. Rare-earth doped sol-gel materials for optical waveguides. *Opt. Lasers Eng.* **2005**, *43*, 341–347. [CrossRef]
13. Scheuner, J.; Raisin, P.; Pilz, S.; Romano, V. Design and realisation of leakage channel fibres by the powder-in-tube method. In Proceedings of the SPIE: Microstructured and Specialty Optical Fibres, Brussels, Belgium, 3 April 2016. [CrossRef]
14. Renner-Erny, R.; Di Labio, L.; Luethy, W. A novel technique for active fibre production. *Opt. Mater.* **2008**, *29*, 919–922. [CrossRef]
15. Di Labio, L.; Luethy, W.; Romano, V.; Feurer, T. *Broadband Emitter Based on a Multiply Re-Doped Fibre*; Internal Report Institute of Applied Physics; University Bern: Bern, Switzerland, 2008.
16. Di Labio, L.; Luethy, W.; Sandoz, F.; Feurer, T. Broadband emission from a multicore fiber fabricated with granulated oxides. *Appl. Opt.* **2008**, *47*, 1581–1584. [CrossRef] [PubMed]

17. Neff, M.; Romano, V.; Luethy, W. Metal-doped fibres for broadband emission: Fabrication with granulated oxides. *Opt. Mater.* **2008**, *31*, 247–251. [CrossRef]
18. Neff, M. Metal and Transition Metal Doped Fibers. Doctoral Thesis, Institute of Applied Physics, University of Bern, Bern, Switzerland, 2010.
19. Pedrido, C. (Inventor) Method for Fabricating an Optical Fiber, Preform for Fabricating an Optical Fiber, Optical Fiber and Apparatus. Patent Nr. WO 2005/102946 A1.
20. Pedrido, C. (Inventor) Optical Fiber and Its Preform as Well as Method and Apparatus for Fabricating Them. Patent Nr. WO 2005/102947 A1.
21. MacChesney, J.; Johnson, D.W., Jr.; Bhandarkar, S.; Bohrer, M.; Fleming, J.W.; Monberg, E.M.; Trevor, D.J. Sol-eel process for optical fiber manufacture. In *Sol-Gel Synthesis and Processing: Ceramic Transactions*; Komarneni, S., Sakka, S., Phule, P.P., Laine, R.M., Eds.; Wiley: Hoboken, NJ USA, 1998; Volume 95, ISBN 978-1-57498-063-9.
22. Wu, F.; Machewirth, D.; Snitzer, E.; Sigel, G.H. An efficient single-mode Nd^{3+} fiber laser prepared by the sol-gel method. *J. Mater. Res.* **1994**, *9*. [CrossRef]
23. Brinker, C.J.; Scherer, G.W. *Sol-gel Science*; Academic Press: Waltham, MA, USA, 1990; ISBN 978-0-12-134970-7.
24. Wu, F.; Puc, G.; Foy, P.; Snitzer, E.; Sigel, G.H. Low-loss rare earth doped single-mode fiber by sol-gel method. *Mater. Res. Bull.* **1993**, *28*, 637–644. [CrossRef]
25. Li, Y.; Huang, J.; Li, Y.; Li, H.; Gu, S.; Chen, G.; Liu, L.; Xu, L. Optical properties and laser output of heavily Yb-doped fiber prepared by sol-gel method and DC-RTA technique. *J. Lightwave Technol.* **2008**, *26*, 3256–3260. [CrossRef]
26. Zang, W.; Wu, J.; Zhou, G.; Xia, C.; Liu, J.; Tian, H.; Liang, W.; Hou, Z. Yb-doped silica glass and photonic crystal fiber based on laser sintering technology. *Laser Phys.* **2016**, *26*, 035801. [CrossRef]
27. Wang, S.; Xu, W.; Lou, F.; Zhang, L.; Zhou, Q.; Chen, D.; Chen, W.; Feng, S.; Wang, M.; Yu, C.; et al. Spectroscopic and laser properties of Al-P codoped Yb silica fiber core-glass rod and large mode area fiber prepared by sol-gel method. *Opt. Mater./Express* **2016**, *6*, 69–78. [CrossRef]
28. He, W.; Leich, M.; Grimm, S.; Kobelke, J.; Zhu, Y.; Bartelt, H.; Jäger, M. Very large mode area ytterbium fiber amplifier with aluminum-doped pump cladding made by powder sinter technology. *Laser Phys. Lett.* **2014**, *12*, 015103. [CrossRef]
29. Ballato, J.; Snitzer, E. Fabrication of fibers with high rare-earth concentrations for faraday isolator applications. *Appl. Opt.* **1995**, *34*, 6848–6854. [CrossRef] [PubMed]
30. Leich, M.; Junst, F.; Langer, A.; Such, M.; Schoetz, G.; Eschrich, T.; Grimm, S. Highly efficient Yb-doped silica fibers prepared by powder sinter technology. *Opt. Lett.* **2011**, *36*, 1557. [CrossRef] [PubMed]
31. Langner, A.; Schötz, G.; Such, M.; Reichel, V.; Grimm, S.; Leich, M.; Unger, S.; Kirchhof, J.; Wedel, B.; Krause, V.; et al. Comparison of silica-based materials and fibers in side- and end-pumped fiber lasers. In Proceedings of the SPIE: Fiber Lasers VI: Technology, Systems, and Applications, San Jose, CA, USA, 24 January 2009. [CrossRef]
32. Wilhelm, B.; Romano, V.; Weber, H.P. Fluorescence lifetime enhancement of Nd^{3+}-doped sol-gel glasses by Al-codoping and CO_2-laser processing. *J. Non-Cryst. Solids* **2003**, *328*, 192–198. [CrossRef]
33. Velmiskin, V.V.; Eqorova, O.E.; Mishkin, V.; Nishchev, N.; Semjonov, S.L. Active material for fiber core made by powder-in-tube method: subsequent homogenization by means of stack-and-draw technique. In Proceedings of the SPIE: Microstructured and Specialty Optical Fibres, Brussels, Belgium, 16 April 2012. [CrossRef]
34. Neff, M.; Romano, V.; Luethy, W. Spectrally flat Co^{2+}:Al^{3+}:SiO_2 fibre attenuator. In Proceedings of the Lasers and Electro-Optics 2009 and the European Quantum Electronics Conference, Munich, Germany, 14–19 June 2009. [CrossRef]
35. Pilz, S.; Etissa, D.; Barbosa, C.; Romano, V. Infrared broadband source from 1000 nm to 1700 nm, based on an Erbium, Neodymium and Bismuth doped double-clad fiber. *ALT Proc.* **2012**, *1*. [CrossRef]
36. Braccini, S.; Ereditato, A.; Giacoppo, F.; Kreslo, I.; Nesteruk, K.P.; Nirkko, M.; Neff, M.; Pilz, S.; Romano, V. A beam monitor detector based on doped silica and optical fibres. *J. Instrum.* **2012**, *7*, T02001. [CrossRef]
37. Dianov, E.M.; Firstov, S.V.; Khopin, V.F.; Alyshev, S.V.; Riumkin, K.E.; Gladyshev, A.V.; Guryanov, A.N. Bismuth-doped fibers and fiber lasers for a new spectral range of 1600–1800 nm. In Proceedings of the SPIE: Fiber Lasers XIII: Technology, Systems and Applications, San Francisco, CA, USA, 13 Feburary 2016. [CrossRef]

38. Dianov, E.M.; Melkumov, M.A.; Shubin, A.V.; Firstov, S.V.; Khopin, V.F.; Guryanov, A.N.; Bufetov, I.A. Bismuth-doped fibre amplifier for the range 1300–1340 nm. *Quantum Electron.* **2009**, *39*, 1099–1101. [CrossRef]
39. Liu, H. Ytterbium-Doped Fiber Amplifiers: Computer Modeling of Amplifier Systems and a Preliminary Electron Microscopy Study of Single Ytterbium Atoms in Doped Optical Fibers. Master Thesis, Department of Engineering Physics, McMaster University, Hamilton, ON, Canada, 2011.
40. Muller, D.A. Structure and bonding at the atomic scale by scanning transmission electron microscopy. *Nat. Mater.* **2009**, *8*, 263–270. [CrossRef] [PubMed]
41. Raisin, P.; Scheuner, J.; Romano, V.; Ryser, M. High-precision confocal reflection measurement for two dimensional refractive index mapping of optical fibers. In Proceedings of the SPIE: Microstructured and Specialty Optical Fibres IV, Prague, Czech, 13 April 2015. [CrossRef]
42. El Sayed, A.; Pilz, S.; Ryser, M.; Romano, V. Two-dimensional refractive index profiling of optical fibers by modified refractive near-field technique. In Proceedings of the SPIE: Optical Components and Materials XIII, San Francisco, CA, USA, 13 Fenurary 2016. [CrossRef]
43. El Sayed, A.; Pilz, S.; Ryser, M.; Romano, V. Two-dimensional refractive index profiling of optical fibers by modified refractive near-field technique. In Proceedings of the SPIE: Microstructured and Specialty Optical Fibres IV, Brussels, Belgium, 3 April 2016. [CrossRef]
44. El Sayed, A. High Spatial-Resolution Optical Time Domain Reflectometer for the Characterization of Doped Optical Fibers. Master Thesis, Institute of Applied Physics, University of Bern, Bern, Switzerland, 2014.